

Hole doping by molecular oxygen in organic semiconductors: Band-structure calculations

Chi-Ken Lu and Hsin-Fei Meng*

Institute of Physics, National Chiao Tung University, Hsinchu, Taiwan, Republic of China

(Received 24 September 2006; revised manuscript received 1 February 2007; published 28 June 2007)

The sensitive effect of O₂ adsorption on the electronic properties of organic semiconductors is investigated by band structure calculation. O₂ can actually *p*-dope the host materials even without illumination, i.e., a ground state property, in the circumstance of saturated coverage. Due to hybridization between O₂ and polymer, Fermi level of the oxygenated system is pinned at the nearly half-filled oxygen band and overlap with host valence band. The doping depends critically on the ionization potential. Each O₂ can dope more than 0.1 hole in dark and a full charge-transfer excitation around 2.3 eV photon energy is predicted.

DOI: 10.1103/PhysRevB.75.235206

PACS number(s): 72.80.Le, 71.55.-i, 72.10.-d

I. INTRODUCTION

Compared with metals and insulators, semiconductors are unique in that their electrical properties can be widely tuned by the dopants. Inorganic semiconductors are usually classified into intrinsic and extrinsic ones depending on the existence of the dopants, and analogy has been made to organic semiconductors. Most of the materials used in organic semiconductor devices are thought to be intrinsic, since no dopant is intentionally incorporated. Yet it is well known that their electrical conductivity is highly sensitive to external conditions despite the materials has been carefully purified. The distinction between intrinsic and extrinsic semiconductors is therefore blurred and questionable. In the past several years it became clear that the gas molecules are responsible for such sensitivity. In particular, the ubiquitous molecular oxygen physically adsorbed to the organic semiconductors is shown to cause a *p*-doping, in sharp contrast to inorganic semiconductors where doping is through chemical bonding with impurity atoms. So far very little is known about the nature of oxygen doping, and apparently the well-established donor/acceptor doping theory of inorganic semiconductor is far from applicable.¹ The high sensitivity to molecular oxygen, or the role of O₂ as a *p*-dopant, has been found in conjugated polymers,²⁻⁴ small molecules,⁴ as well as carbon nanotubes.⁵ From energy conservation, it appears that such doping could be accomplished only with some additional excitation since the ionization potential (IP) of organic semiconductors (between 5 and 6 eV) is usually much larger than the electron affinity (EA) of O₂ (0.45 eV in gas phase⁶). Indeed, the effect of *p*-doping in pentacene field-effect transistor (FET) is apparent only with illumination of UV light.⁴ However, it does not seem so in the case of poly(3-hexyl thiophene) (P3HT) as the current-voltage measurement in dark condition still presents significant off-current.^{3,4} In addition, using poly(3',4'-dialkyl-2,2',5',2''-terthiophene) (PTT) with similar chemical structure but of larger IP as active layer can reduce the off-current.⁷ Thus the *p*-doping can happen in dark, i.e., a ground state rather than excited state property, depending critically on the highest occupied molecular orbital (HOMO) level of the host material.

In this work we clarify theoretically the mechanism of *p*-doping in organic semiconductors for both in dark and under illumination. With a self-consistent tight-binding

scheme which considers the correlation effects on O₂, we can obtain the band structures for a class of oxygenated polythiophene. O₂ is unique in that it has two half-filled molecular orbitals which contribute to its paramagnetism. Through wave function hybridization with the polymer, the oxygen band becomes degenerate with the polymer valence band and Fermi level is pinned by the oxygen band to lie inside the valence band. In other words, the adsorbed O₂ transforms the semiconducting polymer into a metal even at the ground state. Such metal-insulator transition has been predicted for oxygenated single-wall carbon nanotube.^{8,9}

II. BAND STRUCTURE OF POLYTHIOPHENE DERIVATIVES

The chemical structure for a thiophene is shown in the upper panel in Fig. 1. A thiophene contains six π electrons, four of which from carbon atoms and the rest from the sulfur atom. The π band shown in the left panel of Fig. 2 is obtained from a set of tight-binding parameters¹⁰ given by $\epsilon_1 = -1$ eV, $\epsilon_2 = 0$, $\epsilon_s = -3.8$ eV, $t_1 = -2.8$ eV, $t_2 = -3.5$ eV, $t_3 = -2.5$ eV, and $\tau = -3.2$ eV.¹¹ The Fermi level is set at zero. The HOMO level corresponds to the edge state labeled by

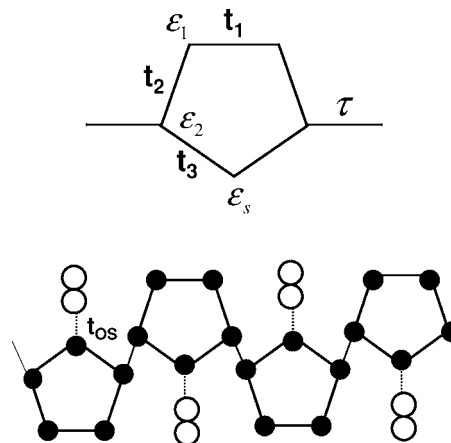


FIG. 1. The upper panel shows the chemical structure for polythiophene and its tight-binding parameters for the π band. The lower panel represents the configuration for the combined system for polythiophene containing the adsorbed O₂ (empty circles).

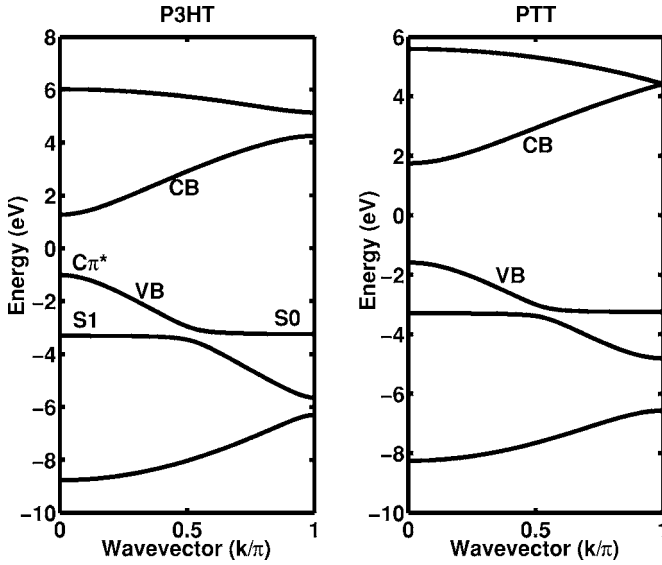


FIG. 2. The π bands for polythiophene with the Fermi level is set at energy zero. The band resulting from larger $|\tau|$ in the left panel shows elevated HOMO level and wider valence bandwidth in comparison to the band with smaller $|\tau|$ in the right panel. We identify the left π band with P3HT while the right with PTT. In fact the IPs are 4.98 and 5.22, respectively, for P3HT and PTT (Ref. 7).

C_{π^*} of the valence band (VB), and their wave functions have most components on the two top carbon atoms with an anti-bonding combination. The two flat parts labeled by S0 and S1 have most components on the sulfur atom. The magnitude of τ , a measure of π delocalization between molecular orbitals on adjacent thiophene units, can alter the position of HOMO. As $|\tau|$ increases, the bandwidth of VB increases and hence the HOMO is elevated. The chemical structure for P3HT causes it to have more planar conformation than PTT since in the latter there are more side-chain repulsions.⁷ Therefore larger $|\tau|$ can be expected in P3HT. Consequently, the right panel in Fig. 2 demonstrates the lowering of HOMO level and the reduction of the bandwidth of VB for the identical tight-binding parameters except τ of -2.2 eV. We identify the left π -bands with P3HT while the right with PTT. The great difference in air stability of these two polymers will be discussed below for illustrating the essence of dark doping by O_2 . In addition, the tight-binding parameter τ also characterizes the trend of band gap among the polythiophene derivatives, as shown in Fig. 3. In other words, the one like P3HT, in the larger $|\tau|$ end, naturally has longer conjugation length and smaller band gap, while the one like PTT has much shorter length and larger band gap. This also qualitatively explains the trend of band gap among conjugated polymers and small molecules.

III. ELECTRONIC STRUCTURE OF OXYGENATED POLYTHIOPHENE

The donor site which interacts with O_2 is the sulfur atom in thiophene for the heteroatom contains a lone pair of electrons¹² and the density of π -electron is highest around it within a thiophene unit cell. Thus the lower panel of Fig. 1 is

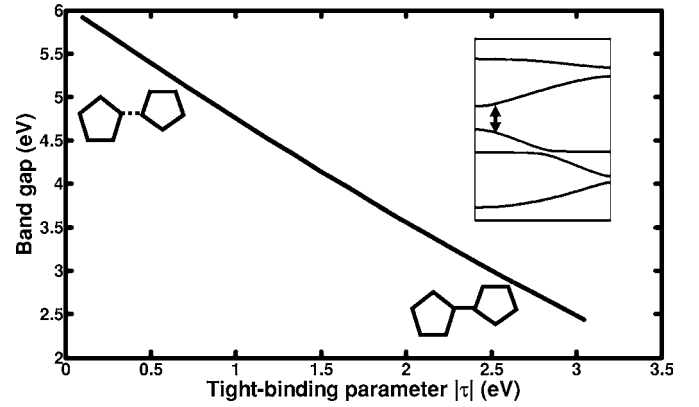


FIG. 3. Variation of band gap, indicated by the arrow in the inset, of polythiophene derivatives with respect to the tight-binding parameter $|\tau|$. The inset at larger $|\tau|$ has a solid line representing a stronger connection among adjacent thiophene units, while at the lower end the thiophene units are connected by a dashed line, implying the connection is weak and resulting in a shorter conjugation length. This figure can also explain the trend of band gap among the conjugated polymers and small molecules, which usually have much shorter length.

to represent the oxygenated polythiophene. In addition, each thiophene unit is attached by one O_2 to simulate high-density adsorption. The wave functions for the π band are composed of p_z atomic orbitals as we regard the plane for thiophene as the x - y plane, and they have the odd inversion symmetry with respect to the thiophene plane. On the other hand, taking the O_2 bond as y axis, the O_2 molecule has its two valence electrons occupying the two degenerate molecular orbitals π_x^* and π_z^* . According to Fig. 1, only π_z^* has nonvanishing coupling with the π band due to symmetry. We can regard the combined system as a thiophene chain weakly interacting with an infinity number of π_z^* states from those adsorbed gas molecules. As in the case of single-wall carbon nanotube,⁸ the combined system has an additional half-filled band associated with the oxygen π_z^* .

The following Hamiltonian H_0 for an isolated O_2 is considered:

$$H_0 = \sum_{\alpha=\{x,z\}\sigma} \left(\xi a_{\alpha\sigma}^\dagger a_{\alpha\sigma} + \frac{U}{2} n_{\alpha\sigma} n_{\alpha-\sigma} \right) - \frac{J}{2} \vec{S}_{\pi_x^*} \cdot \vec{S}_{\pi_z^*}, \quad (1)$$

where π_x^* and π_z^* have their creating(annihilating) operators labeled by $a_\alpha^\dagger(a_\alpha)$ and the spin operator \vec{S}_{α^*} . ξ stands for the on-site energy for the degenerate levels. The positive U term refers to the direct Coulomb repulsion when two electrons occupying the same orbital. Here the exchange effect in the Coulomb interaction is included in the effective spin-spin interaction term with positive prefactor J which gives the paramagnetic spin-triplet ground state for O_2 . The values for U and J can be obtained by the definition of EA and IP for O_2 in the gas phase.¹³ $(2\xi - \frac{J}{2}) + IP = \xi$ and $(3\xi + U) + EA = 2\xi - \frac{J}{2}$. Note that the vacuum is set as energy reference. $2\xi - \frac{J}{2}$ is the ground state energy for 3O_2 . ξ is the energy of an ionized O_2 . $3\xi + U$ is the energy for O_2^- . The difference between singlet and triplet configurations gives J of 1 eV.⁸ Hence the

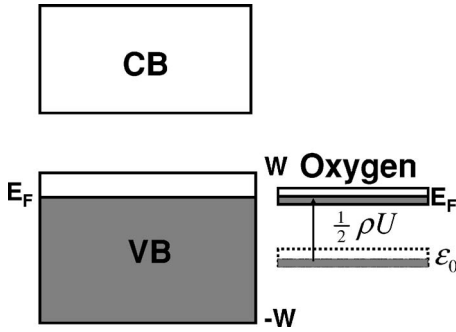


FIG. 4. Schematic plot for valence and conduction bands for organic semiconductor. Due to electron transferred to O_2 , the oxygen band is shifted upward as a result of increasing Coulomb repulsion.

repulsion $U = IP - EA - J = 10.6$ eV and the on-site energy $\xi = -11$ eV. ξ is to be scaled to fit the reference of the host material.

In an isolated O_2 , the spins of the two electrons in the π_z^* and π_x^* orbitals are in triplet configuration due to the strong Coulomb correlation. However once the density of the adsorbed O_2 is so high that an O_2 band is formed through hybridization with the polymer π bands, the oxygen wave functions become delocalized Bloch state and the spin correlation is no longer important. We can then treat the highly oxygenated polymer in a spin-independent fashion and ignore the exchange interaction. Because of the hybridization, the expectation value of the electron occupation in each O_2 is no longer fixed at 2 as in the isolated molecule. The O_2 on-site energy depends on the occupation number due to Coulomb repulsion. Therefore we define the on-site energy for π_z^* orbital of spin σ as $\varepsilon_{\sigma} = \xi + U \langle n_{-\sigma} \rangle$ where $n_{-\sigma}$ represents the occupation operator for electron of opposite spin on the same orbital.¹⁴ $\langle \dots \rangle$ is the ground state expectation value. Hence the actual on-site energy has to be determined self-consistently if additional electrons occupying the orbital. For later convenience we define the on-site energy for free oxygen band as $\varepsilon_0 \equiv \xi + U/2$, which corresponds to a level below vacuum by 5.8 eV. This number corresponds to the mean-field on-site energy when there is no electron transfer.

The weak hybridization between the oxygen π_z^* and sulfur atomic orbitals here can split the bands from its unperturbed ones and allow electrons transferring to O_2 . The ultimate band structure, with consideration of the correlation effects, is obtained as follows. We first consider the case of P3HT. When P3HT is isolated from the O_2 chain, the top of valence band lies above the oxygen band because P3HT has an IP of 5 eV while the oxygen band lies below vacuum by 5.8 eV as indicated by ε_0 in Fig. 4. Once the coupling t_{OS} is turned on, the electrons occupying the top of valence band may transfer to the lower oxygen band, which cause a lift of oxygen band according to its on-site energy as shown by the arrow in Fig. 4. The positions of Fermi level and the flat oxygen band, which depends on the occupance on π_z^* , have to be determined in a self-consistent manner. Here we take advantage of the narrowness of the oxygen band to have a simpler way determining both positions. Since the flat oxygen band can neither be empty nor filled because O_2 has a large IP and a

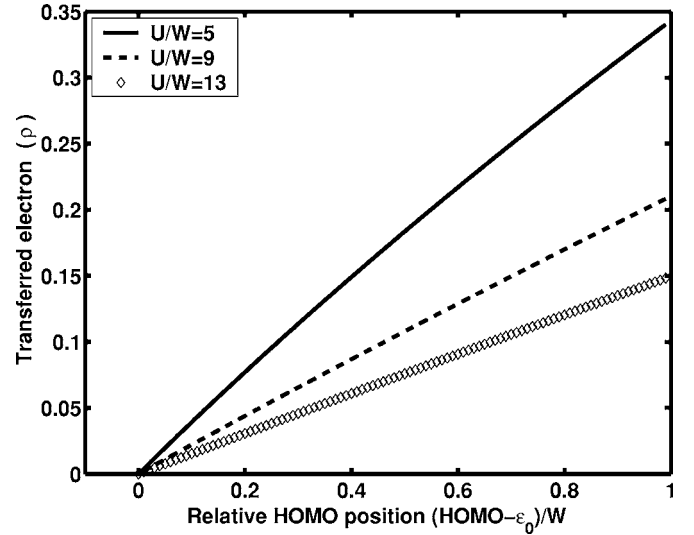


FIG. 5. The relation between the transferred electron ρ per unit cell and the position of host HOMO level.

small EA, Fermi level must be pinned with the flat band in order to keep the π_z^* having an occupation not far from unity on average, i.e., a nearly half-filled oxygen band. Though the perturbation t_{OS} can widen the oxygen band slightly, its bandwidth is small. If we neglect the perturbation due to the weak coupling t_{OS} , the position of the flat band is solely determined by the π_z^* on-site energy. Thus the Fermi level can be given by a simple relation

$$E_F = \varepsilon_0 + \frac{\rho}{2} U, \quad (2)$$

where ρ is the density of electron transferred to O_2 . Note that for less dense adsorption, the basic picture in Fig. 4 remains the same and we only have to modify Eq. (2) to meet the fact that each electron given up by the polymer now has to be shared by fewer adsorbed O_2 . Therefore the prefactor $U/2$ for ρ in Eq. (2) must be multiplied by a factor to account for the missing density of O_2 . Below we consider the dense adsorption depicted in Fig. 1. According to Eq. (2) the number of transferred electrons ρ , lifting the oxygen band as shown in Fig. 4, has to coincide with the number of empty states between the valence band edge and Fermi level. If we set the center of valence band as reference and approximate its dispersion as $\varepsilon(k) = W \cos k$, then the transferred electron density is given by

$$\rho = \frac{2}{\pi} \cos^{-1} \left(\frac{E_F}{W} \right). \quad (3)$$

Therefore ρ can be obtained by solving Eqs. (2) and (3) with the given dimensionless on-site energy ε_0/W and Coulomb repulsion U/W . As shown in Fig. 5, as long as the HOMO level lies above the center of free oxygen band ε_0 , the density of transferred electron ρ is nonzero. Note that the resultant ρ is surely small due to the large U . Therefore E_F must locate just below the valence band edge, at which a high density of states exists. Hence only the band edge is important for determining the unknown ρ , which in turn justifies

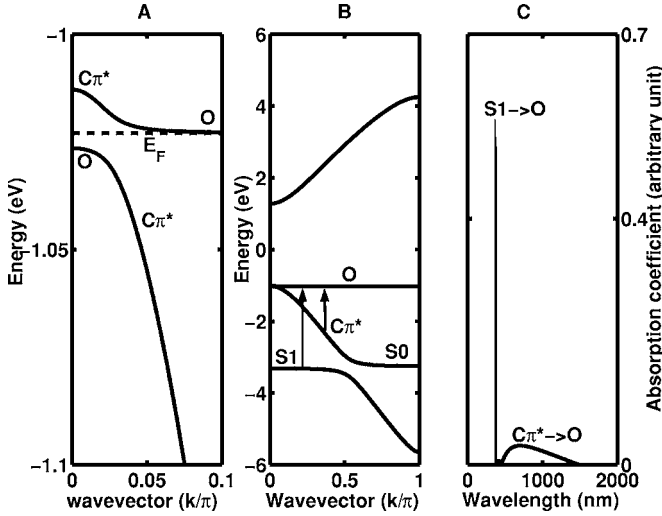


FIG. 6. (A) Partial band structure near the Fermi level (dashed line) for oxygenated P3HT. The free holes occupy the states labeled by $C\pi^*$. (B) The oxygen band is degenerate with the valence band edge. (C) Absorption due to photon excitation in the oxygenated P3HT.

our use of a cosine band which also possesses the same density of state near the band edge.

The weak coupling t_{OS} perturbs more significantly the bands which have larger components on sulfur and oxygen atoms. Therefore, the oxygen band and the segments $S0$ and $S1$ are mixed with nonzero t_{OS} . The value of t_{OS} can be obtained by $\frac{1}{4\pi\epsilon} \int d^3\mathbf{r} \varphi(\mathbf{r}) \frac{1}{r} \phi(|\mathbf{r}-\mathbf{d}|)$, where the wave functions φ and ϕ , respectively, stand for the p_z orbitals on sulfur and oxygen atoms in Fig. 1. d is the separation between them and it can be determined by estimating the adsorption potential with Lennard-Jones 6-12 form in which the attraction part, from dipole-dipole interaction, is assumed to be a function of polymer band gap.¹⁶ In this way we have $t_{OS} = -0.2$ eV.

IV. RESULTS AND DISCUSSIONS

The resultant π -band structure is shown in Fig. 6 with $\rho = 0.15$ for the oxygenated P3HT in Fig. 1. ϵ_0/W and U/W are, respectively, 0.27 and 9.6 and Fermi level $E_F/W = 0.97$ lies just below the edge of valence band. Hence the oxygenated P3HT is a metal where free hole carriers exist. Despite the hybridization with O_2 , the wave functions of $C\pi^*$ valence band edge still have the dominate contribution from carbon p_z orbital. The nature of the holes is identical with the holes on a pristine polymer without O_2 . On the other hand, holes in the oxygen band can hardly move due to the very large effective mass. This is consistent with the experimental finding that the average hole mobility is decreased by the oxygenation.² This transformation from intrinsic semiconductor to metal by adsorbed O_2 explains the effect of O_2 p doping in dark. Note that such doping occurs even at zero temperature, in contrast to the n/p doping for inorganic semiconductors where small thermal energy is required to lift the carriers to the bands. Moreover, O_2 act collectively in-

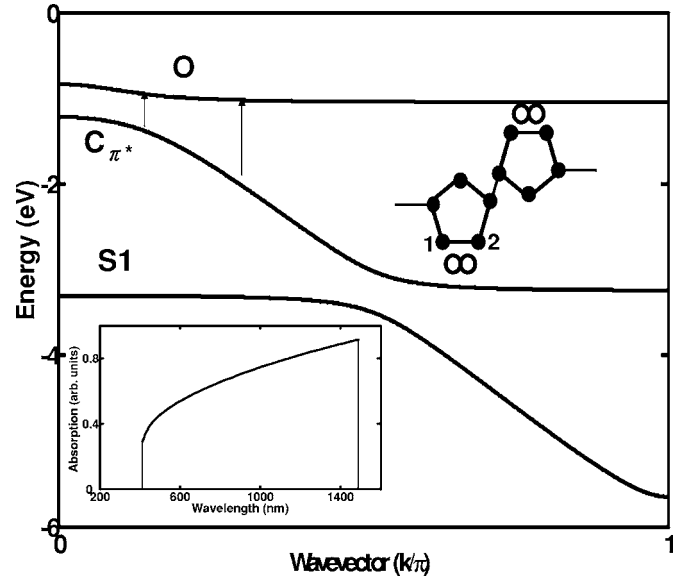


FIG. 7. Resultant band structure for the configuration in which the carbon atoms, labeled by 1 and 2 in the upper inset, act as donor site for O_2 adsorption. The predicted absorption spectrum in arbitrary unit, as shown in the lower inset, is different from that in Fig. 6(c). The choice of donor site interacting with the adsorbed O_2 is crucial regarding the absorption spectra. See the text for more details.

stead of giving its own hole individually as in inorganic semiconductors. In addition to the empty states near $C\pi^*$ at ground state, photons can excite the electrons in the sulfur band and the valence band to the empty states on the oxygen band.

The optical transition coefficient α is given by

$$\alpha \sim |\langle f|p|i\rangle|^2 \rho_j. \quad (4)$$

It is proportional to the square of the matrix element of the momentum operator p and the joint density of state ρ_j between the initial state $|i\rangle$ and the final states $|f\rangle$. Since the final state is the oxygen state, only the sulfur atom on the polymer has a significant optical transition matrix element. So the transition coefficient is proportional to the square of the sulfur component of the initial state and the joint density of state. The relative absorption spectrum is shown in the right panel of Fig. 6. The sharp peak at 2.3 eV (400 nm) is from the sulfur band, while the broad tail is from the valence band. Both the large sulfur component and the large joint density of state of the $S1$ to O transition marked in Fig. 6(b) contributes to the peak shown in Fig. 6(c). This result is remarkably consistent with the experiment.² The sharp peak implies a optical transition between two narrow bands. Our calculation verifies not only that the corresponding initial state is the occupied $S1$ band, but the fact that there are comparable number of adsorbed oxygen molecules providing the empty π_z^* levels.

We repeat the calculation for the configuration, as shown in the inset of Fig. 7, in which the carbon atoms act as the donor site interacting with the adsorbed O_2 . In this case, the coupling between π_z^* and carbon atomic levels can be written

as $t_{OC}(a_{\pi_z^*}^\dagger a_1 - a_{\pi_z^*}^\dagger a_2)$, where a_1^\dagger and a_2^\dagger corresponds to the creation operators of atomic levels on carbon 1 and 2 in the inset of Fig. 7. The minus sign appears because of the anti-binding character of $O_2 \pi_z^*$. It gives a similar band structure which is expected since the oxygen band is still a flat one pinned near the valence band edge by the same reasoning. The distortion of oxygen band is still negligible since the coupling with carbons t_{OC} is weak in comparison with other tight-binding parameters. However the photoexcitation is different. In this case the photo excitation has its largest matrix element between the empty oxygen band states and the occupied Bloch states with character of C_{π^*} . Therefore the spectrum in the inset of Fig. 7 corresponds to the optical transition from the broader valence band. The key difference is the missing of a sharp peak corresponding to transitions from a narrow bandwidth of states to oxygen band near the wavelength of 400 nm in the previous configuration. Since the peak is a key experimental signature,² our configuration appears to be more appropriate.

Reducing $|\tau|$ can lower the HOMO position and alter the p -doping significantly. For example, polythiophene with IP larger than 5.8 eV such as PTT in Fig. 2, the additional oxygen band will lie slightly above the valence band. The p doping in dark is significantly suppressed by the large IP, but a photoinduced p -doping is possible. Obviously we can generalize the O_2 doping dependence on IP to other organic semiconductors. For small molecules such as pentacene with IP of 6 eV,¹⁵ the off-current for pentacene FET is apparent only under both illumination and O_2 exposure,⁴ in complete agreement with our prediction.

As stated above a single O_2 is not able to reconcile the picture for such p -doping because of its low EA. Consider a weak coupling for the single O_2 and assume the organic semiconductor were p -doped by it, the Fermi level would go down and touch the edge of valence band and generate one free hole. Once this took place, the lost electron would occupy nowhere but the O_2 , which however took exceedingly high energy as indicated by the small EA. Therefore a cluster of adsorbed O_2 , as in the lower panel of Fig. 1, is required to accept the additional electron. In addition, the free hole carrier density has been quantitatively extracted from the pinch-off voltage of P3HT FET,³ and the carrier density actually rises only after a sufficiently long time of O_2 exposure, say 1 h. This observation supports that doping in the dark has a threshold adsorption density for the cluster formation. In other words, the assumption of saturation adsorption of oxygen molecules is again justified.

Oxygenation is also expected to modify the metal interface dramatically. The fact that Fermi level is pinned by the flat oxygen band is of crucial importance when the organic material is in contact with metal. Naively, Fermi level is fixed by the metal and can be anywhere within the band gap of organic semiconductor. However, for the oxygenated organic semiconductors, the adsorbed O_2 contributes a band within the band gap which pin the Fermi level of metal by its high unoccupied density of state. This is consistent with the observation of different barrier heights for exposed and unexposed carbon nanotube FET's.¹⁷ For titanyl phthalocyanine (TiOPc), the fact that Fermi level is fixed about 0.6 eV above its HOMO for various metal contacts¹⁸ is also consistent with such concept.

Before drawing the conclusion, we would like to comment the effect of disorder in this case. In practice, the presence of disorder can generate a few localized states in the band gap. Under the assumption of saturation adsorption the wave function hybridization between O_2 and the polymer, leading to transfer of electrons to O_2 , remain the same since most of those states within the band are not perturbed significantly by the disorder. However, as the density of adsorbed O_2 is low and comparable to the defect density, oxygen will favor adsorption on the defect trap states and the effect will be sensitive to the level of disorder which cause the trap states.¹⁶

V. CONCLUSION

In conclusion we establish a model for the p -doping mechanism of polythiophene derivatives by physically adsorbed molecular oxygen based on a self-consistent tight-binding scheme. We believe that such model could be generalized to other organic semiconductors which are susceptible to the oxygen adsorption. Due to the hybridization of O_2 and polymer, Fermi level is pushed into the valence band and pinned with the oxygen band due to charge transfer to O_2 . The doping depends on the oxygen density in a highly nonlinear way. We found a quantitative relation between the amount of transferred electron and the ionization potential of the host materials. A wide range of experiments on the effect of air exposure for organic semiconductors can be well explained by this theory.

ACKNOWLEDGMENT

This work is supported by the National Science Council of Taiwan, R.O.C.

*Electronic mail: meng@mail.nctu.edu.tw

¹B. A. Gregg, S. G. Chen, and R. A. Cormier, Chem. Mater. **16**, 4586 (2004).

²M. S. A. Abdou, F. P. Orfino, Y. Son, and S. Holdcroft, J. Am. Chem. Soc. **119**, 4518 (1997).

³E. J. Meijer, C. Detcheverry, P. J. Baesjou, E. van Veenendaal, D. M. de Leeuw, and T. M. Klapwijk, J. Appl. Phys. **93**, 4831

(2003).

⁴S. Ogawa, T. Naijo, Y. Kimura, H. Ishii, and M. Niwano, Jpn. J. Appl. Phys., Part 1 **45**, 530 (2006).

⁵P. G. Collins, K. Bradley, M. Ishigami, and A. Zettl, Science **287**, 1801 (2000).

⁶R. G. Tonkyn, J. W. Winniczek, and M. G. White, Chem. Phys. Lett. **164**, 137 (1989).

- ⁷B. Ong, Y. Wu, L. Jiang, P. Liu, and K. Murti, *Synth. Met.* **142**, 49 (2004).
- ⁸S. H. Jhi, S. G. Louie, and M. L. Cohen, *Phys. Rev. Lett.* **85**, 1710 (2000).
- ⁹S. Dag, O. Gülseren, T. Yildirim, and S. Ciraci, *Phys. Rev. B* **67**, 165424 (2003).
- ¹⁰C. Coulson and R. Mallion, *Hückel Theory for Organic Chemists* (Academic, London, 1978).
- ¹¹*Organic Electronic Materials, Conjugated Polymers and Low Molecular Weight Organic Solids*, edited by R. Farchioni and G. Grosso (Springer, Berlin, 2001).
- ¹²*Handbook of Photochemistry and Photobiology*, edited by H. S. Nalwa (American Scientific Publishers, New York, 2003), Vol. 2: Organic Photochemistry.
- ¹³*CRC Handbook of Chemistry and Physics*, 79th ed., edited by D. R. Lide (CRC, Boca Raton, FL, 1998/1999).
- ¹⁴J. R. Schrieffer, *J. Vac. Sci. Technol.* **9**, 561 (1971).
- ¹⁵H. Y. Chen and I. Chao, *Chem. Phys. Lett.* **401**, 539 (2005).
- ¹⁶C. K. Lu, S. T. Pi, and H. F. Meng, *Phys. Rev. B* **75**, 195206 (2007).
- ¹⁷V. Derycke, R. Martel, J. Appenzeller, and Ph. Avouris, *Appl. Phys. Lett.* **80**, 2773 (2002).
- ¹⁸T. Nishi, K. Kanai, Y. Ouchi, M. R. Willis, and K. Seki, *Chem. Phys.* **325**, 121 (2006).